A novel hybrid floating breakwater- WEC device: preliminary experimental investigations

Sara Russo, Claudio Lugni, Pasquale Contestabile and Diego Vicinanza

Abstract—**The marine space is increasingly emerging as an optimal contender to drive the economic growth of the energy sector, given its vast reserves of natural resources like waves, wind and solar energy. Different devices harnessing these marine renewables have been thought to be assembled in a new concept of an energy hub for the Mediterranean Sea, recently proposed by the National Research Council of Italy.**

The successful implementation of this ambitious floating energy archipelago heavily relies on the creation of a sheltered sea area with reduced wave heights. To address this need, a specially designed floating breakwater module has been developed to surround the energy hub, potentially with multiple rows.

Furthermore, an intriguing possibility is being explored to use this floating module for both its traditional dissipative function and as a wave energy converter. This dual-purpose implementation presents a significant technical challenge as it requires optimising both functionalities through adjustments in the module's draft.

This study presents preliminary results obtained from experimental tests carried out on a 1:10 Froude-scaled model. The dynamic behaviour of the hybrid device is evaluated in terms of response amplitude operators, while wave attenuation performances are assessed by the transmission coefficient, indicating the reduction in wave height within the energy hub.

Keywords— **Draft varying floater, hybrid floating breakwater-WEC, laboratory testing, Mediterranean Sea, multi-use device.**

I. INTRODUCTION

The increasing demand for clean energy is boosting the renewable energy sector, in which marine renewable energies are assuming an even crescent role because of the enormous amount of spaces and resources to be exploited.

In order to tap into the vast potential of the blue energy market in the Mediterranean Sea and create technologies that can be globally deployed, it is crucial to develop solutions that are specifically optimized for this enclosed basin [1]. Amidst the array of stand-alone systems and blue energy farms, a novel concept has emerged to enhance offshore energy harvesting in the Mediterranean region: the Floating Energy Archipelago, recently proposed by the Institute of Marine Engineering of the Italian National Research Council. Originally designed for deep-sea areas characteristic of the Mediterranean Sea, the energy archipelago represents a pioneering approach to a floating smart city. It operates autonomously in terms of energy, harnessing renewable marine resources such as solar, wind, and geothermal energy. These sources are utilized to generate liquid fuels (such as methanol and/or hydrogen) through fuel cells, as well as to power energy-intensive processes like seawater desalination and aquaculture activities. This integrated system presents a sustainable and multifaceted solution for meeting the energy needs of coastal regions in the Mediterranean and beyond.

The archipelago, is protected by an external multiarray of floating modules with the dual functionality of:

- extract energy from the waves.
- function as a breakwater, favoring a reduction of the wave field in the indoor area.

For this purpose, a floating breakwater module, drawing simultaneously inspiration from the Salter's Duck [2] and the traditional naval hull, has been specifically designed to surround the archipelago with one or more rows. Moreover, investigating the possibility to implement a dual and alternative use of this floating module, as a traditional dissipative system and wave energy converter has resulted in an extremely challenging task. With respect to the existing hybrid floating breakwater-Wave Energy Converters in fact, the novelty of this device is the optimization of both functionalities by varying its draft. In extremely rough seas, the hybrid module should only serve as a passive breakwater, soaking up incoming waves and safeguarding the

This work is part of the "Ricerca di Sistema" project (RSE, 1.8 "Electricity from the Sea") founded by Italian Ministry of the Environment, Land and Sea.

S.R., P.C and D.V. are with the Università degli Studi della Campania "L.Vanvitelli", via Roma, 29 Aversa (CE) - 81031, Italy (e-mail: sara.russo@unicampania.it, diego.vicinanza@unicampania.it pasquale.contestabile@unicampania.it,)

C.L. is with the Institute of Marine Engineering, CNR-INM, Via di Vallerano, 139 Roma – 00128 Italy (e-mail: claudio.lugni@cnr.it)

Digital Object Identifier: https://doi.org/10.36688/ewtec-2023-318

equipment installed inside the archipelago. Otherwise, the floating module should operate as a WEC in more frequent mild sea states, assisting the archipelago's energy output. The whole produced energy can be stored and used to supply the development of new productive activities, such as aquaculture, the expensive process of seawater desalination, as well as the production of low environmental impact fuels like methanol or hydrogen.

Since the proposal of the first wooden floating breakwater in 1811 for protecting the Plymouth Sound [3], these unconventional coastal defenses [4] have garnered increasing interest, especially among wave energy operators, that could integrate their solution in reliable and cost-effective substructures, even in low-energy seas [5]-[6]-[7].

Presently, hybrid floating breakwaters are classified based on the type of wave energy converter (WEC) system, as discussed in a comprehensive review by Zhao et al., 2019 [8]. One type of WEC system is the oscillating water column, which features a hollow structure. Examples of such devices can be found in [9]-[10]-[11]-[12], incorporating one or more air chambers equipped with air turbines for electricity generation. While these studies have demonstrated the potential of these devices to function as WECs, their primary purpose remains coastal protection due to their relatively low energy conversion efficiency. Another proposal by Michailides & Angelides, 2011 [13], introduced a flexible floating breakwater comprising multiple modules connected by a power take-off (PTO) system driven by the relative motion of the modules.

Box-type breakwaters utilizing "wave-activated bodies" or "oscillating bodies" as WECs have also reached the stage of engineering application [14]. Pile-restrained floating breakwaters with integrated PTO systems [15] have been investigated as well. The performance evaluation of these devices has been conducted using linear potential flow theory [16]. Although they have a lower technological readiness level, they exhibit greater potential for dual-purpose applications. However, a significant drawback is the substantial long-wave attenuation under operational conditions.

A potential solution lies in coupling WECs on the weather side of floating breakwaters [17]-[18]-[19]-[20]-[21]. This arrangement offers improved efficiency, often employing arrays of smaller modular WECs compared to the breakwater behind them. Furthermore, the presence of the rear breakwater causes wave reflection, thereby amplifying the motion of the WECs and leading to increased efficiency of the WEC array [22].

The present work preliminarily analyses the results obtained in an experimental campaign on a 1:10 Froude-scaled module carried out in the wave tank of the Department of Engineering of Università degli Studi della Campania "L. Vanvitelli". In particular, the dynamic behavior of the hybrid device is evaluated in terms of response amplitude operators, while the attenuation performances are condensed in the transmission coefficient which indicates the reduction of the wave height inside the archipelago. Section 2 describes both the device and the experimental set-up while section 3 reports the main results and includes a comparison with a 3D BEM numerical model. Section 4 instead, deals with discussions and general conclusion, underlying the next steps aimed at further developing the device.

II. Materials and Methods

A. The device

The innovative hybrid system object of this work, moving from the existing solutions integrating floating breakwater and wave energy converter, was first presented in [23]. However, several adjustments have been required to improve its assembly and functionality [24].

In fact, the main feature of this device is its adjustable draft that enables a dual function, as passive breakwater, or wave energy harvester. Depending on the sea-state condition, the draft of the floater can be modified to alter the overall stability. In extreme and severe sea-states, the device primarily serves as a passive breakwater, absorbing the incoming waves and protecting the devices installed within the archipelago. Conversely, in more frequent mild sea states, the floating device operates as WEC, contributing to the energy production of the archipelago. In this case, the maximum energy is harvested when the floating module resonates with the waves.

The FB-WEC design involved a longitudinally-developing truncated lower cylinder, connected to an upper trapezoid. The reference system was centred on the keel line of the device, as depicted in Fig. 1, with the free surface tangent to the keel. When adjusting the draft, the free surface is conceptually imagined as moving along the positive z-axis.

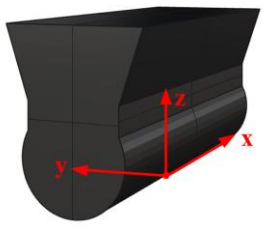

Fig. 1. Origin of the coordinate system.

Since only the lower part of the module directly interacts with waves in the wave energy converter condition, the cylinder shape was chosen to maximize motion exploitation. Experimental and numerical studies in fact, [25] confirmed that the cylinder configuration exhibited large peak-to-peak roll amplitudes with smaller

values of added mass moment of inertia [26]. On the other hand, in the breakwater condition, enlarging the body surface interacting with waves enhances stability.

Different operational conditions were analysed by considering two values of the draft obtained by gradually ballasting the model, respectively D1= 1.25 m and D2=2.5m, as shown in Fig. 2. This variation resulted in different stability conditions, directly related to the ability of the module to move, and hence generate waves.

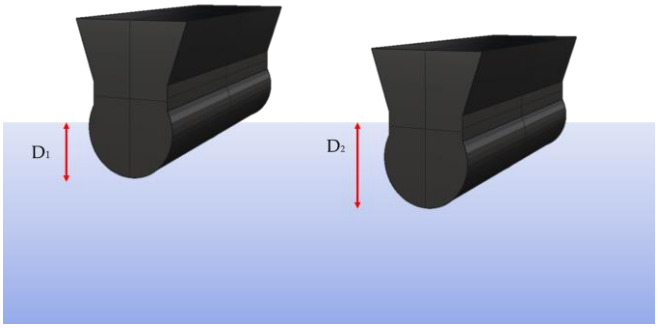

Fig. 2. Sketch of the laboratory tested drafts. Left: D_1=1.25 m, right: D_2=2.5m.

The transverse metacentric height GM_T is the most representative stability parameter for the proposed device. It is defined as the distance between the vertical centre of gravity and the metacentre [27]. As shown in Fig. 3, where the transversal section of a generic floater is represented, the metacentre is denoted as MT and is a fictious point intersecting the vertical lines passing respectively from the centre of gravity, G, and the centre of buoyancy, B.

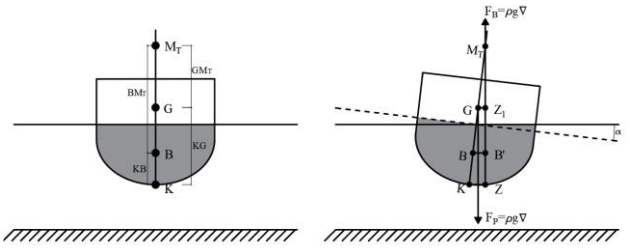

Fig. 3. Stability parameters identification. Left: at equilibrium, right: under heel angle.

For small heel angles, up to 10, the GM_T can be assumed as constant and to follow eq.1:

$$GM_T = \mathrm{KB} + BM_T - \mathrm{KG} \quad (1)$$

where BM_T represents the distance from the metacentre to the centre of buoyancy B, also called metacentric radius; KB is the distance from the keel to centre of buoyancy; and KG is the distance from the keel to the centre of gravity G. These parameters depend on the shape of the hull and on the amount and distribution of the weights. When adjusting the draft, D, these parameters change due to variation sin weight and submerged volume (hereinafter displacement ∇).

For the WEC functioning of the device, the metacentric height has been chosen equal to 0.2 m for both drafts. Then, the centre of gravity has been derived by means of eq. 1.

TABLE I
GEOMETRIC AND PARAMETRIC PROPERTIES

Symbol	Quantity	Unit
L	Total length	10 m
R	Radius of the lower cylinder	1.5 m
H	Total height	5 m
B	Total beam	4 m
r_{xx}, r_{yy}, r_{zz}	Gyradii of inertia	1.4 m; 2.5 m; 2.5 m
D_i	Drafts	1.25 m; 2.5 m
B_w	Waterline Beams	2.96 m; 2.65 m
GM_T	Transverse metacentric height	0.2 m; 0.2 m
KG	Centre of gravity from Keel	1.30 m; 1.41 m
∇	Displacement	27.83 m^3; 63.42 m^3

B. *Experimental set-up*

To accurately simulate the behaviour of the model as wave energy converter (WEC), a Foude-scaled 1:10 model was constructed and tested in laboratory. The model was assembled using four PVC sheets, with two sheets forming the side profiles and two sheets creating the trapezoidal shapes. Additionally, a cylindrical section of the same 4mm thick PVC material was utilized.

For the upper part of the model, the PVC sheet covered only one third of the available surface. This design choice aimed to facilitate manual ballasting and de-ballasting operations and reduce inertia. Furthermore, perforated bars were mounted on the side sheets to serve as connection points for the anchoring system. As the 1:10 scale model was specifically designed to test WEC conditions, understanding its dynamics is crucial to assess its effectiveness. When the wave and the device approach resonance in fact, the maximum energy can be harnessed. It is also important to measure the transmission coefficient. Two different draft values were investigated: D_1=0.125m and D_2=0.25m. The key geometric and inertial characteristics of the floating platform for both drafts of the 1:10 model are summarized in Table II.

TABLE II
PLATFORM PROPERTIES

Symbol	Quantity	Unit
R	Radius of the lower cylinder	0.15 m
D_i	Drafts	0.125 m; 0.25 m
G	Centre of gravity from SWL	0.01 m; -0.104 m
M_{TOT}	Mass, including ballast	27.83 kg; 63.42 kg
I_{44}	Roll inertia	0.24 kg·m^2; 0.54 kg·m^2
I_{55}, I_{66}	Pitch and Yaw inertia	1.74 kg·m^2; 3.96 kg·m^2

The mooring system components instead, are described in Table III. Specifically, the module was secured using four lines, two in the front and two in the back of the model, each connected to a gravity anchor positioned on the ground. As depicted in Figure 4, each

line consisted of a 1m inextensible rope, connected to a system of four springs [28], and followed by a load cell. Finally, the load cell was connected to the model through a 70cm long flexible steel cable.

TABLE III
MOORING PROPERTIES

Quantity	Unit
Number of mooring lines	4
Vertical angle starboard-rear	120°
Horizontal angle starboard-rear	180°
Depth to anchors below SWL	1.55 m
Depth to fairleads below SWL	1.45 m;1.38 m
Radius to anchors from platform centreline	3.25 m
Number of springs per line	4
Spring Pretension	0.7 kg
Unstretched spring length	1.16 m
Stretched spring length	1.37 m
Equivalent springs extensional stiffness	0.033 N/mm
Stretched mooring line length	3.58 m;3.53 m

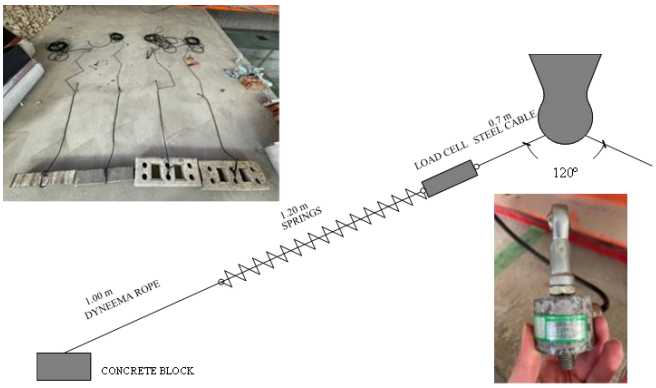

Fig. 4. Mooring lines arrangement.

C. Test Facility and Instrumentation

The experimental investigations were carried out in the three-dimensional tank of the Department of Engineering of University of Campania "L. Vanvitelli", whose section is shown in Fig. 5. The tank measured 16m parallel to the wave paddle and 12m in the perpendicular direction, with a depth ranging from 0.9m to 0.43m. A dissipative beach was constructed in the final section, while a deeper area was created in the middle. The last measured 5.50 m by 6.50 m respectively parallel and perpendicular to the wavefront, with depths varying from 1 m to 1.30 m. The overall average depth of the tank when filled with water was 1.4-1.8 m.

The experimental campaign aimed to achieve two main objectives: evaluating the dynamic behavior of the device and assessing its hydraulic performance in waves. To evaluate the device's dynamic behavior, an inertial measurement unit (IMU) was used, which measured accelerations, angular velocities, and inclinations along the three axes [29]. Additionally, submersible in-line load cells were attached to each mooring line to measure the tension resulting from wave forces [30]. The wave profile was recorded using six resistive wave gauges, with three located in front of the model to measure wave reflection based on the Mansard and Funke method [31], two placed behind the model to measure wave transmission, and one positioned outside the tank to compare internal and external measurements. Regular waves were generated using the AwaSys software developed at the Hydraulics and Coastal Engineering Laboratory of the University of Aalborg (Denmark) [32]. For data acquisition, three different software tools were employed: "WaveLab2" for recording the wave profile elevation [33], the software provided with the IMU sensor for capturing the device's movements, and a LabVIEW code [34] for recording the tension in the mooring lines using the load cells. All acquired data, sampled at a frequency of 20 Hz, were synchronized, processed, and analyzed using MATLAB.

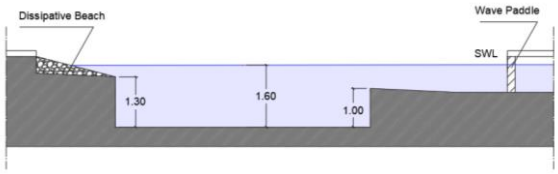

Fig. 5. Wave tank section.

D. Experimental test program

The first part of the experimental test program was related to the calibration of the model in the two draft conditions. With the models properly identified, its behaviour under wave loads was examined, in terms of response amplitude operators and transmission coefficient.

1) Model Calibration

In order to achieve the desired characteristics of the model, such as the draft, the KG, the centre of gravity, the mass and the inertia, several steps were taken. Initially, the model was weighed without any ballast, and its centre of gravity and natural periods in pitch and roll were determined. Subsequently, preliminary tests were conducted after placing the model in water. These tests included measurements of the static draft, trim, and heel. Inclining tests were performed for each draft value to calculate the transverse metacentric height (GM_T). This was achieved by measuring the angle of inclination obtained when a known mass (m) was moved to different positions (Δy), and the stability parameter was determined by solving eq. 2. Once the model was adjusted to the desired values of draft, trim, heel, and design weight, the roll inertia was evaluated by measuring the angular frequency in water (eq. 3).

$$m \cdot \Delta y = \rho \cdot \nabla \cdot GM_T \cdot sin(\alpha) \tag{2}$$

$$\omega_{Roll} = \sqrt{\frac{\rho \cdot g \cdot \nabla \cdot GM_T}{I_{Roll} + A_{Roll}}} \tag{3}$$

Static tests were performed to evaluate the moored

model's restoring characteristics. The mooring system was initially pre-tensioned at 0.7 kg while the model was in its mean position. Subsequently, the model underwent a series of quasi-static displacements along the positive and negative y-axis at equidistant intervals, and the corresponding mooring tensions were measured and recorded.

Free oscillation tests were conducted on the moored model in the six degrees of freedom (surge, sway, heave, roll, pitch, yaw) to determine the natural periods and damping coefficients. The natural periods T_N in particular, for each DoF were obtained by averaging the n-th cycles taken by the device to decay (eq. 4).

$$T_{N,j} = \sum_{i=1}^{n} T_i \tag{4}$$

2) Response under regular waves

Regular wave tests with constant steepness ka=0.075, according to Table IV, were performed to evaluate both the dynamic behaviour and the attenuation performances of the device with the two values of the draft, as shown in Fig. 6.

TABLE IV
REGULAR WAVE TESTS

ka [-]	Tp [s]	Hs[m]
0.075	0.6	0.01
	0.8	0.02
	1	0.04
	1.2	0.05
	1.4	0.07
	1.6	0.10

In particular, the dynamic response was evaluated by defining the response amplitude operators (RAOs) of the motion, as in eq. 5, where ξi represents the i-th DoF depending on the angular frequency ω, and a the wave amplitude. Also the mooring response was evaluated by deriving the response amplitude operators, obtained from the tensions T recorded by the load cells (as in eq. 6). Finally, the transmission coefficient was determined by dividing the wave amplitude occurring behind the model by the one registered in front of it, both recorded by means of resistive a wave gauges (eq. 7).

$$RAO_{\xi_i} = \frac{|\xi_i(\omega)|}{a} \tag{5}$$

$$RAO_{T_i} = \frac{|T(\omega)|}{a} \tag{6}$$

$$K_T = \frac{a_T}{a_I} \tag{7}$$

(a)

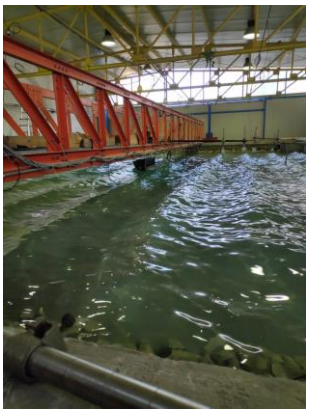

(b)

Fig. 6. Model floating in regular waves. (a) Draft 1; (b) Draft 2.

E. Numerical model

The Response Amplitude Operators obtained from the experimental tests carried out on the 1:10 model were then compared with the ones derived from the resolution of the boundary value problem by means of an in-house 3D- BEM (boundary element method) numerical solver based on the linear potential flow theory. In particular, being the RAO for each DoF given by eq. 5, the complex amplitude of the motion $\xi_i(\omega)$ is here obtained by solving the equation of motion in frequency domain (eq. 8).

$$[-\omega^2(M + A(\omega) + i\omega B(\omega) + K] \cdot \xi(\omega) = F(\omega) \tag{8}$$

In eq. 8, M and A(ω) are respectively the structural mass and the added mass matrixes, B(ω) is the radiation damping coefficient matrix, K is the restoring coefficient matrix and F(ω) is the vector of the excitation forces.

Due to the linearity assumption of the problem, which allows the decomposition of the fluid-dynamic problem [35] into two sub-problems, the added mass and the damping coefficients matrixes can be derived from the resolution of the radiation problem, while the exciting forces con be derived from the diffraction one.

III. RESULTS

F. Model calibration

The mass and the inertia moments of the empty model were initially determined in air with a measured mass of 11.72 kg (Fig. 7a). Afterwards, the floater was properly ballasted in water to achieve the desired centres of gravity and the design drafts, with zero trim and heel. Subsequently, inclining tests were conducted to determine the transverse metacentric height of the device in its different draft configurations (Fig. 7b). As designed, the last parameter was 0.02m for both D_1 and D_2.

(a) (b)

Fig. 7. Model calibration. (a) Mass and Inertia measurements; (b) Transverse metacentric height identification.

G. *Free Decay Tests*

In order to assess the natural periods and damping coefficients, free decay tests were conducted in still water. The results in terms of natural periods and their corresponding standard deviations are reported in Table V. It is important to note that these results were obtained with the model equipped with the mooring system.

TABLE V
NATURAL PERIODS

	Tm D_1	std D_1	Tm D_2	std D_2
Surge	11.28 s	1.28 s	16.61 s	0.16 s
Sway	5.13 s	0.60 s	8.61 s	0.16 s
Heave	0.74 s	0.00 s	1.11 s	0.09 s
Roll	2.19 s	0.40 s	1.54 s	0.03 s
Pitch	1.27 s	0.31 s	1.27 s	0.03 s
Yaw	3.11 s	0.04 s	4.63 s	0.20 s

H. *RAOs*

Fig. 8 presents the Heave and Roll Response Amplitude Operators (RAOs) of the model in regular waves, plotted against the ratio λ/B_w, where λ represents the wavelength. The RAOs correspond to regular waves with a constant steepness of ka=0.075, as indicated in Table IV. For both degrees of freedom, it is evident that the highest response peak occurs when the wave periods are near the natural periods of the structure, indicated with the dashed lines, respectively for each DoF. The results are shown for both D_1(a)-(b) and D_2(c)-(d) cases.

I. *Transmission Coefficient*

The transmission coefficient was calculated for the two draft values, considering a constant wave steepness ka=0.075. The results are presented, respectively for draft 1 and draft 2 in Fig. 10. (a) and (b). For the first value of the draft, KT reaches its maximum value of 0.9 with the shortest wave period, indicating the effectiveness of the module in generating waves. As the wave period (and height) increases, the transmission coefficient decreases, reaching a minimum value of 0.45 for T=1.6s. On the other hand, a different behaviour is observed for the second draft value. The transmission coefficient starts from a minimum of 0.1 for the shortest waves and gradually increase, reaching a maximum value near the roll natural period of 1.6s for the D_2 case. In general, it is evident that the wave lengths tested were relatively short compared to the beam of the module for both drafts, and it is well known that floating breakwaters perform exceptionally well in short waves.

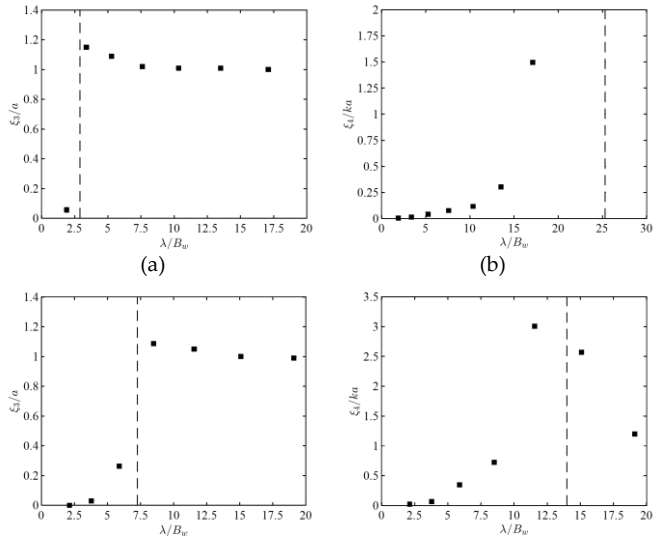

(a) (b) (c) (d)

Fig. 8. Response Amplitude Operators of Heave and Roll for Draft 1 (a)-(b) and Draft 2 (c)-(d).

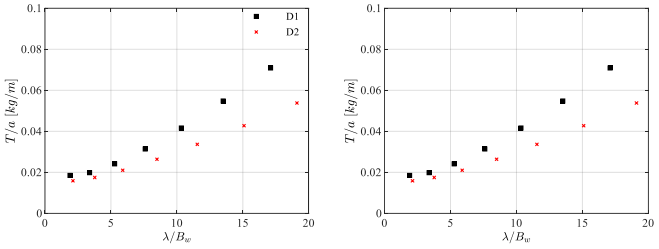

(a) (b)

Fig. 9. Response Amplitude Operators of mooring lines tensions: (a) Starboard line, (b) rear line.

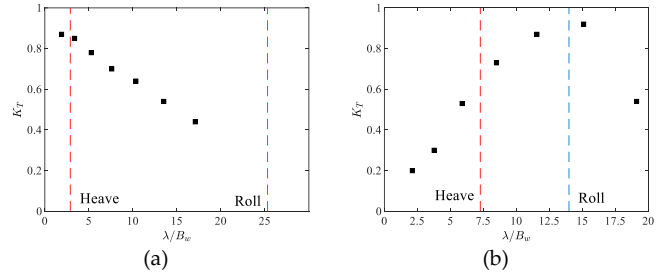

(a) (b)

Fig. 10. Measured transmission coefficient: (a) Draft 1, (b) Draft 2.

J. *Comparison with numerical results*

As there is the necessity to analyse different scenarios, numerical codes that could properly simulate the wave-structure interaction problem have to be assembled. As preliminary feedback, the experimental dynamic response of the FB-WEC in scale 1:10 was compared to numerical results obtained using an in-house BEM code based on the linear potential flow theory. In particular, the results in terms of heave and roll response amplitude

operators are reported in Fig 11. It can be noticed that numerical and experimental data are in agreement; however, the numerical prediction overestimates the response. When in proximity of the resonant $\lambda/$ the discrepancies between predicted and measured values are higher.

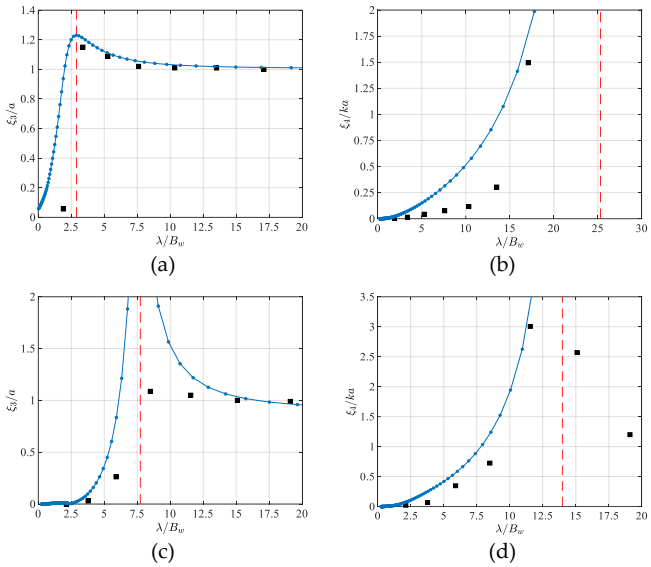

Fig. 11. Numerical Response Amplitude Operators of Heave and Roll for Draft 1 (a)-(b) and Draft 2 (c)-(d).

IV. Discussions, Conclusions and Future Works

This work introduces an innovative hybrid floating breakwater-wave energy converter that has been tested in the wave tank of the Department of Engineering at the University of Campania "Luigi Vanvitelli". The uniqueness of this hybrid device lies in its optimized dual functionality as both wave energy converter and a floating breakwater, achieved by adjusting its draft. The performance of this device has direct implications for the practical implementation of a floating energy archipelago, as it aims to reduce wave agitation during severe wave conditions. Conversely, in more frequent mild sea states, the floating module is intended to function as a wave energy converter, contributing to the energy production of the archipelago. This study focuses on a 1:10 model, properly scaled to test the WEC functioning of the device, with two different draft values, investigating its dynamic response, mooring line tensions, and transmission coefficient. Furthermore, the experimental Response Amplitude Operators (RAOs) of the motions are compared to the numerical results obtained using an in-house Boundary Element Method (BEM) code.

The evaluation of heave and roll motion RAOs reveals that, for both draft values, the response peak occurs when the wave periods align with the corresponding natural periods of the structure. Analysing the mooring tensions, which are calculated by dividing tension by wave amplitude, it is observed that they slightly increase with the wavelength for all draft values, both for the starboard and rear lines. These curves exhibit a gentle slope because the mooring response is expected to reach a peak near the sway natural period, which has been intentionally designed to be significantly higher than wave periods, gradually increasing from D1 to D2. Additionally, the transmission coefficient has been estimated, demonstrating a strong dependence on the natural period of the structure. As the structure approaches the resonance periods of roll and heave motion, the transmission coefficient increases, reaching its maximum values of 0.87 for D_1 and 0.92 for D_2. Notably, in the case of the first draft value, the transmission coefficient is highest for the lowest λ/B_w value and decreases with increasing λ/B_w. A qualitative explanation for this behaviour can be attributed to the exceptional wave generation capability of the floater. The analysed wave condition, representative of a mild sea state in the Mediterranean Sea for the 1:10 scale model ($\lambda \simeq 40$m), confirms the functioning of the wave energy converter, especially for D_2. Overall, this study on the innovative floating breakwater-wave energy converter validates its potential in protecting multi-use offshore platforms, reducing wave loads on each component, and supplying electricity by converting wave energy.

The results of this work underscore the importance of further developing the hybrid module, as its optimization will significantly impact the feasibility of the energy archipelago. The initial step towards achieving this objective is the creation of a hybrid numerical-laboratory environment that incorporates non-linearities and allows for scaling up the devices. Regarding the individual module, a primary future upgrade focuses on selecting a Power-Take-Off (PTO) system. The analysis of existing PTO systems' efficiency and operating mechanisms suggests that a gyroscopic system or an integrated sloshing/Oscillating Water Column (OWC) system is a suitable choice. This decision is crucial because the energy conversion mechanism directly affects the device's dynamics, and different PTO systems can lead to significant variations.

References

[1] Azzellino, A., Lanfredi, C., Riefolo, L., De Santis, V., Contestabile, P., & Vicinanza, D. (2019). Combined exploitation of offshore wind and wave energy in the Italian seas: a spatial planning approach. Frontiers in Energy Research, 7, 42.

[2] Salter, S. H. (1974). Wave power. Nature, 249(5459), 720-724.

[3] Stuart, W., 1842. On the Plymouth breakwater. In: Report of the 11th Meeting of the British Association for the Advancement of Science. John Murray, London.

[4] Contestabile, P., Crispino, G., Russo, S., Gisonni, C., Cascetta, F., & Vicinanza, D. (2020). Crown wall modifications as response to wave overtopping under a future sea level scenario: An experimental parametric study for an innovative composite seawall. Applied Sciences, 10(7), 2227.

[5] Permanent International Association of Navigation Congresses (PIANC), Floating Breakwaters: A Practical Guide for Design and Construction, 1994. [Online] Available online: https://www.pianc.org/publications/marcom/floatingbreakwaters-a-practical-guide-fordesign-and-construction (accessed on 10 January 2021).

[6] Majidi, A., Bingölbali, B., Akpınar, A., Iglesias, G., & Jafali, H. (2021). Downscaling wave energy converters for optimum performance in low-energy seas. Renewable Energy, 168, 705-722.

[7] Contestabile, P., Russo, S., Azzellino, A., Cascetta, F., & Vicinanza, D. (2022). Combination of local sea winds/land breezes and nearshore wave energy resource: Case study at MaRELab (Naples, Italy). Energy Conversion and Management, 257, 115356.

[8] Zhao, X. L., Ning, D. Z., Zou, Q. P., Qiao, D. S., & Cai, S. Q. (2019). Hybrid floating breakwater-WEC system: A review. Ocean engineering, 186, 106126.

[9] Neelamani, S., Natarajan, R., Prasanna, D.L., 2006. Wave interaction with floating wave energy caisson breakwaters. J. Coast. Res. 22 (2), 745–749.

[10] Koo, W., 2009. Nonlinear time–domain analysis of motion-restrained pneumatic floating breakwater. Ocean Eng. 36 (9), 723–731.

[11] He, F., Leng, J., Zhao, X., 2017. An experimental investigation into the wave power extraction of a floating box-type breakwater with dual pneumatic chambers. Appl. Ocean Res. 67, 21–30.

[12] Sundar, V., Moan, T., Hals, J., 2010. Conceptual design of owc wave energy converters combined with breakwater structures. In: ASME 2010 29th International Conference on Ocean, Offshore and Arctic Engineering.

[13] Michailides, C., Angelides, D.C., 2011. Wave energy production by a flexible floating breakwater. In: Proceedings of the 21th International Offshore and Polar Engineering

[14] Com, M., 2017. Breakwater Beats the Weather at Holy Loch. https://www.maritimejournal.com/news101/marine-civils/port,-harbourandmarineconstruction/breakwater_beats_the_weather_at_holy_loch.

[15] Ning, D., Zhao, X., Goteman, M., Kang, H., 2016. Hydrodynamic performance of a pile-restrained wec-type floating breakwater: an experimental study. Renew. Energy 95, 531–541.

[16] Zhao, X., Ning, D., Zhang, C., Kang, H., 2017. Hydrodynamic investigation of an oscillating buoy wave energy converter integrated into a pile-restrained floating breakwater. Energies 10 (5), 712.

[17] Zingale, G., 2002. Modular Floating Breakwater for the Transformation of Wave Energy.

[18] Martinelli, L., Ruol, P., Favaretto, C., 2016. Hybrid structure combining a wave energy converter and a floating breakwater. In: Proceedings of the International Offshore and Polar Engineering Conference, 2016, 2016-January, pp. 622–628.

[19] Favaretto, C., Martinelli, L., Ruol, P., Cortellazzo, G., 2017. Investigation on possible layouts of a catamaran floating breakwater behind a wave energy converter. In: Proceedings of the 27th International Offshore and Polar Engineering Conference.

[20] Ning, D., Zhao, X., Zhao, M., Kang, H., 2018. Experimental investigation on hydrodynamic performance of a dual pontoon–power take-off type wave energy converter integrated with floating breakwaters. Proceedings of the institution of mechanical engineers, Part M. Journal of Engineering for the Maritime Environment, 1475090218804677.

[21] Ning, D.Z., Zhao, X.L., Chen, L.F., Zhao, M., 2018. Hydrodynamic performance of an array of wave energy converters integrated with a pontoon-type breakwater. Energies 11 (3), 685.

[22] Zhao, X.L., Ning, D.Z., Liang, D.F., 2019. Experimental investigation on hydrodynamic performance of a breakwater-integrated wec system. Ocean Eng. 171, 25–32.

[23] Russo, S., Lugni, C., Contestabile, P., Vicinanza, D. (2021). A Preliminary Design for a novel concept of Floating breakwater (… and WEC). Proceedings of the 14th European Wave and Tidal Energy Conference, 5-9 Sept 2021, Plymouth, UK, ISSN 2309-1983.

[24] Russo, S., Contestabile, P., Lugni, C., & Vicinanza, D. Experimental Investigation on a Draft Varying Floating Breakwater-Wave Energy Converter for Offshore Protection. Under Review.

[25] Clemente, D., Rosa-Santos, P., Taveira-Pinto, F., & Martins, P. (2022). Experimental performance assessment of geometric hull designs for the E-Motions wave energy converter. Ocean Engineering, 260, 111962.

[26] Clemente, D., Rosa-Santos, P., Taveira-Pinto, F., & Martins, P. (2021). Influence of platform design and power takeoff characteristics on the performance of the E-Motions wave energy converter. Energy Conversion and Management, 244, 114481.

[27] Techet, A.H. Hydrodynamics for Ocean Engineers; MITPRESS: Cambridge, MA, USA, 2004.

[28] https://dim.molle.com/dettagli.asp?id=533

[29] https://www.wit-motion.com/digital-inclinometre/witmotion-wt901c-ttl-9-axis-imu-sensor.html (Accessed on: November 2021)

[30] https://appmeas.co.uk/products/load-cells-force-sensors/in-line-submersible-load-cell-dden/ (Accessed on: March 2022)

[31] Mansard, E. P., & Funke, E. R. (1980). The measurement of incident and reflected spectra using a least squares method. Coastal Engineering Proceedings, (17), 8-8.

[32] Meinert, P., Andersen, T. L., & Frigaard, P. (2011). AwaSys 6 user manual.

[33] Frigaard, P., & Andersen, T. L. (2014). Analysis of waves: Technical documentation for wavelab 3.

[34] https://www.ni.com/it-it/about-ni.html (Accessed on: December 2021)

[35] Faltinsen, O. (1993). Sea loads on ships and offshore structures (Vol. 1). Cambridge university press.